Active and Passive Seismic Investigations in the Coso Geothermal Field, Eastern California

Satish Pullammanappallil[1], William Honjas[1], Jeffrey Unruh[2] and Francis Monastero[3]

[1]Optim LLC, University of Nevada, Reno
[2]William Lettis & Associates, Inc., Walnut Creek, CA
[3]Geothermal Program Office, China Lake NAWC, CA

Keywords

Seismic reflection imaging, micro-earthquakes, seismic velocity inversion and optimization

ABSTRACT

During December of 1999, approximately 45 km of multichannel seismic reflection data were acquired within the Coso Geothermal Field, Inyo County, California, as part of a detailed seismic investigation being undertaken by the US Navy Geothermal Program Office (GPO). As part of Phase 1 of the project (2000-2001), the seismic reflection data along individual 2D lines were processed and velocity models and reflection images derived showing several interesting structures. To confirm these structures and to derive further information contained in the data, GPO funded Phase 2 of the project. The goal of this phase was to produce a detailed 3D-velocity model of the area encompassing the geothermal field. Active source seismic data was combined with micro-earthquake data in a joint hypocentral-velocity inversion in order to improve the depth of resolution of the velocity model. Another goal of the study was to increase the understanding of the relationship between seismic velocities and the location of permeable structures within the Coso geothermal field. The proposed work builds on a study funded by the US Navy Geothermal Program Office (USNGPO, Contract Number: N68936-99-C-0186) that involved acquiring and processing new 2D seismic data within the Coso geothermal field (William Lettis & Associates and Optim LLC, 2001). Phase 3 of the project will involve using the refined velocity models developed during Phase 2 to re-migrate the in-line data and improve the reflection images obtained during Phase 1.

Introduction

Approximately 45 km of reflection seismic data were acquired in the central Coso Range during December 1999 (Figure 1). The goals of the project included the following objectives: constraining the down-dip geometry of tectonic structures that have been mapped at the surface by previous workers; characterizing features that are potentially significant for evaluating subsurface permeability; and, imaging deeper structures and assessing their relationship to faults and fractures controlling reservoir production. In this paper we discuss the techniques used, demonstrate the effectiveness of the technique with a synthetic example, present the results of processing the data from the seismic lines, and compare them to the results obtained using conventional petroleum-type seismic data processing techniques.

During Phase 1 of the project, seismic data collected along the receiver lines were processed using a combination of detailed velocity modeling using the simulated annealing opti-

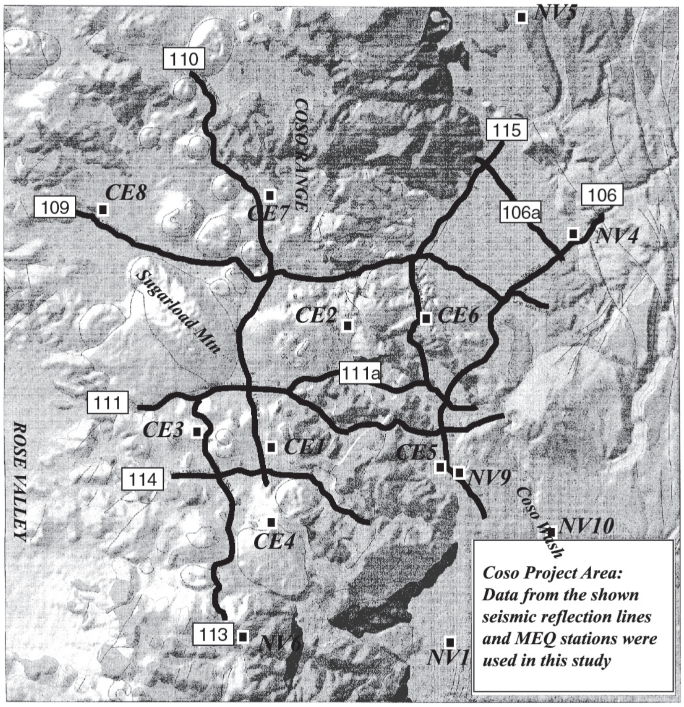

Figure 1. Geologic map of the study area showing the seismic reflection lines and MEQ stations, data from which were used for this study.

mization method and Kirchhoff pre-stack migration to obtain accurate, depth-migrated images of the subsurface structure (Pullammanappallil et al., 2001). The purpose of this phase was to demonstrate the effectiveness of integrated seismic data acquisition and processing techniques for 2D and 3D imaging of structures controlling permeability within the Coso geothermal field. During Phase 2, both in-line (along receivers) and off-line (data from fan shots) were used to generate a true 3D velocity model. This model was then extended in depth using P- and S-wave arrivals picked off micro-earthquake (MEQ) data contained in the Coso MEQ catalog starting from 1995. During Phase 3, the refined velocity model was then used in a 2D Kirchhoff pre-stack migration to improve the depth images obtained during Phase 1.

Methods Used

Two advanced processing techniques were used to process this data set. A nonlinear optimization method, called simulated annealing, was used to derive high-resolution velocity models from seismic first arrivals picked off raw data. These models were then used in a pre-stack Kirchhoff depth migration to directly image subsurface structures. The following sections briefly describe the techniques

Simulated Annealing Velocity Optimization

Simulated annealing is a Monte-Carlo based estimation process that can match P-wave (or S-wave) arrival times to a velocity model even where sophisticated non-linear inversion methods may fail (Pullammanappallil and Louie, 1993; Pullammanappallil and Louie, 1994a). The algorithm works by randomly perturbing an arbitrary starting model until the synthetic seismic wave travel times computed through it match the travel times picked from the new data. New models producing less travel time error are accepted for further enhancements, and models having increased error can be accepted conditionally based on their total error. As annealing proceeds, conditional acceptance becomes less and less likely. Unlike linear, iterative inversions, simulated annealing optimization will find the global velocity solution while avoiding local error minima, thus ensuring the user ends up with the best possible velocity model. The algorithm 'tests' several thousand models before arriving at the most optimal solution. This extensive sampling of the model space guarantees that the final solution is a velocity model that best fits the picked first arrival travel time data. It is also completely insensitive to the starting velocity model, removing the interpreter bias that may be involved in a prospect or project. We used SeisOpt® @2D™ and SeisOpt® @3D™ (© Optim LLC, 2004) commercial software's that incorporates this algorithm, to obtain the velocity models for this project. By employing Optim's proprietary cluster computing technology, the optimization is speeded up considerably. This enabled run times to be practical for large data sets like the one collected at Coso. The same algorithm was also used to obtained 3D velocity models from joint velocity-hypocentral inversion of micro-earthquake data (Asad et al., 1999; Pullammanappallil and Louie, 1994b).

Pre-stack Kirchhoff Migration

The second technique used for processing the data is a Kirchhoff pre-stack depth migration. In the Kirchhoff pre-stack migration imaging procedure, unsorted seismogram traces are mapped into a depth section by computing the travel time from the source to the depth point and back to the receiver for each source-receiver pair, through the velocity model. The travel time calculation includes turning rays, which allows for the imaging of structures that dip away from the seismic source and receivers by undershooting. To allow for wave propagation through a model with lateral velocity heterogeneity, the travel time calculation could take the form of ray tracing through a variable-velocity medium (Louie and Qin, 1991). Once the travel times down to and up from every point in the data volume have been obtained, the value of the seismogram at each time is summed into the depth section. Coherent and continuous events for each time will constructively interfere, indicating the presence of a seismically reflective earth structure at depth. The tomographic sum, or the summation of arrival times, may be made in any order, as the Kirchhoff summation method embraces the geometrical configuration of the source, receiver, and reflector as a function of time. The Kirchhoff pre-stack migration does not require definition of ray path. The ability to calculate travel times from Vidale's (1988) method for laterally heterogeneous structures avoids the limitations of straight ray approximations. The summation of the value of each seismogram, or the amplitudes, at specified times will produce images of structures that cause lateral variations in velocity. As part of the pilot study in Dixie Valley, we have shown that in the presence of well constrained velocities, the pre-stack migration can image basin stratigraphy, steeply dipping faults, and basalt layers (Honjas et al., 1997).

Summary of Phase 1 Results

During Phase 1, 2D velocity models and depth migration sections were obtained using only the in-line data (Figure 1). Figure 2 shows the velocity model obtained along Line 109, which traverses west to east across the geothermal producing region. The velocity model reveals several interesting features. It shows velocity variations across faults with surface expression, such as the Coso Wash fault as well maps the lower velocity sediments that makes up the Coso Wash. The most interesting feature seems to be the relatively lower velocities that underlie the geothermal producing region (between station 130 and station 190). This region is bound by relatively higher velocity region. The model also shows shallowing of higher velocities beneath the topographic high. Within the region bound by the higher velocity blocks, the velocities show lateral and vertical variations. This could be due to fracturing and hydrothermal alteration of the rocks associated with the geothermal activity. In order to image the structures directly we use this velocity model, in conjunction with the reflection data, and perform a Kirchhoff pre-stack depth migration (Figure 3).

Based on analysis and interpretation of the seismic data, we identify three major sets of reflectors in the upper 4 km of the crust (Unruh et al., 2002):

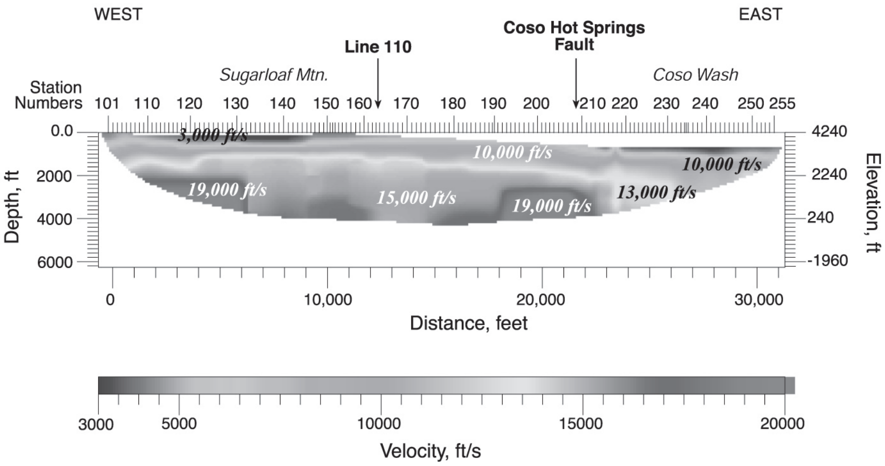

Figure 2. Velocity model obtained from optimization of first-arrival picks recorded along seismic reflection Line 109. The velocity model reveals lateral velocity variations corresponding to the geothermal production zone and sub-surface projection of known faults.

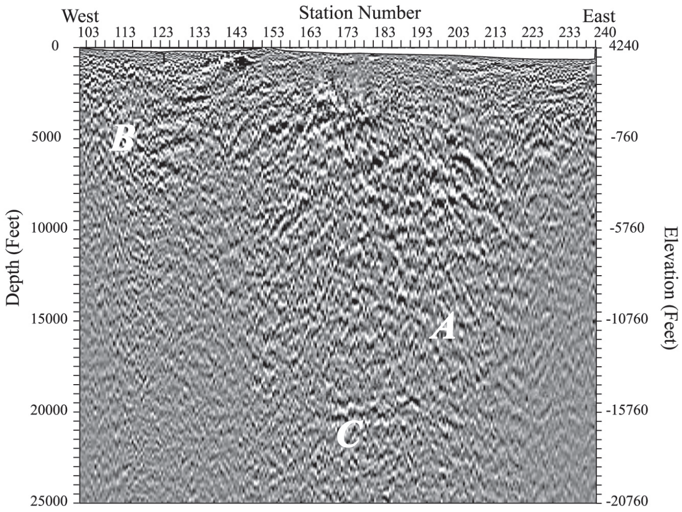

Figure 3. Pre-stack depth migration along Line 109 using the velocity model along Figure 2. The imaging shows a strong reflector (referred to as "C") at depth of 6 km. It also shows a sub-horizontal reflector "A" at about 4 km and southeast dipping reflectors.

1) A series of listric reflectors that dip southeast beneath the geothermal field. The listric reflectors exhibit a left-stepping geometry and are offset in a left-lateral sense by northwest-striking faults. We determined the true strike and dip of the listric reflectors from their geometry in crossing 2D seismic lines, and correlate them with northeast-striking, southeast-dipping faults mapped in the vicinity of the field by Whitmarsh (1997). The Joshua Ridge fault, located south of the seismic array, is a southeast-dipping fault that displaces an intrusive contact approximately 1000 m down to the southeast (Walker and Whitmarsh, 1998), and may be an example of the listric structures beneath the field imaged by the reflection data.

2) Northwest-dipping reflectors that are primarily confined to the hanging walls of the southeast-dipping listric faults. We correlate these features with northeast-striking faults that are expressed by northwest-facing bedrock scarps, and which show evidence for late Quaternary west-down displacement.

3) A subhorizontal reflective zone that underlies the entire seismic array at a depth of about 4 km. For convenience, we refer to this feature as the "A" reflector. In general, microseismicity is confined to the upper crust above the A. Approximately 95% of all seismicity beneath the Coso production area occurs at depths shallower than 4 km (Figure 4).

Four percent of the remaining events occur at depths of 4-4.5 km and only one percent occurs at depths greater than 4.5 km. The base of the seismogenic zone deepens dramatically east and west of the production area to 8-10 km. Following Monastero and Unruh (2002), we interpret that the A reflector is the brittle-ductile transition. Alternatively, the A may be a zone of shearing or a high-pressure fluid-bearing zone that marks the top of the semi-permanent upper boundary of ductile flow beneath the geothermal field.

The seismic data image a high-amplitude reflector at a depth of about 6 km beneath the northern part of the Coso geothermal field. The reflector is slightly convex or antiformal in the plane of the seismic section. For convenience, we refer to this feature as the "C reflector" (Figure 4). The "C" is spatially associated with a low velocity zone at 6 km depth beneath the Coso field imaged by recent passive source studies of crustal structure in this region (Wilson et al., in review). Based on analysis of converted phases from teleseismic events, the 6 km

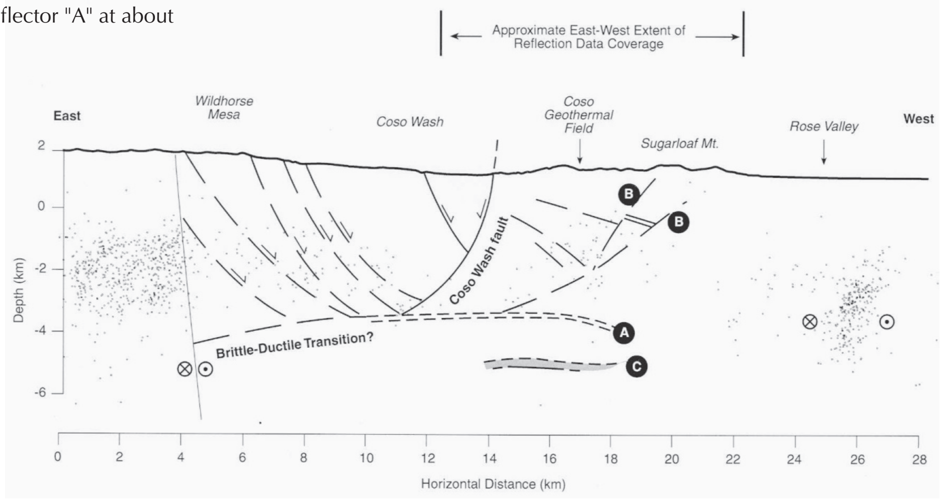

Figure 4. Cross-section through the northern part of study area showing interpretation derived from the depth images obtained during Phase 1. MEQ recorded by the Coso MEQ network (dots) shows the relationship between major structures and background seismicity.

low velocity zone is a strong S-wave converter, which indicates the likely presence of fluids or partial melt. Wilson et al. (in review) interpret the low velocity zone to be the top of a mid-crustal magma chamber that underlies the Coso geothermal field in the depth range of about 6-15 km.

Summary of Phase 2 Results

Data processing was performed in two stages. The first stage involved picking first-arrivals recorded by the active source seismic reflection survey. Both in-line and off-line data were picked. These were then used to construct a 3D velocity model using a non-linear optimization technique called simulated annealing. The second stage of the processing used the near-surface velocity model derived from the first-arrivals as a constraint in a joint hypocentral-velocity inversion using micro-earthquake (MEQ) data contained in the Coso MEQ catalog starting from 1995. Only stations and events that were within the bound of the reflection survey were used in this study (Figure 1). An initial reference model for the three-dimensional inversion was developed using the program VELEST. This uses the Joint Hypocentral Determination (JHD) approach to simultaneously determine earthquake locations and adjustments to a model consisting of the one-dimensional (1-D) velocity structure and a suite of station corrections. This 1-D model was then used in SIMULPS12 to obtain model of the three-dimensional velocity structure in the Coso. SIMULPS12 uses P and S-P arrival times to determine a set of perturbations to apply to the starting model. The resulting updated model is folded back into a new inversion until several convergence parameters are met. A "pseudo-bending" approximate ray tracer is used to determine the travel time of rays through the volume of crust under the array. Although the program solves for the 3D variation in phase velocity the resulting model represents an average over a large volume of crust. The layering used in the program is laterally homogenous. The resulting model was then used as input into a nonlinear optimization algorithm based on the simulated annealing algorithm. This took into account lateral and vertical velocity variations and resulted in a velocity model down to a depth of 13,000 feet.

Selected slices from the 3D volume using the first-arrival optimization are shown in Figure 5. Selected depth slices 3D velocity model obtained from joint velocity-hypocentral location is shown in Figure 6. Using MEQ data allows the 3D model to be extended in depth. In addition one can draw the following inferences:

1. 3D velocity model confirms the southeast dipping features inferred from the reflection images obtained during Phase 1.
2. Low Vp associated with geothermal production area.
3. Low Vp*Vs associated with geothermal production area. According to Lees and Wu (2000) this is a good indicator of higher porosity and could be a useful signature for geothermal exploration.
4. Relatively low Vp/Vs ratios within the geothermal production zone - possible an indicator of presence of elevated temperatures.

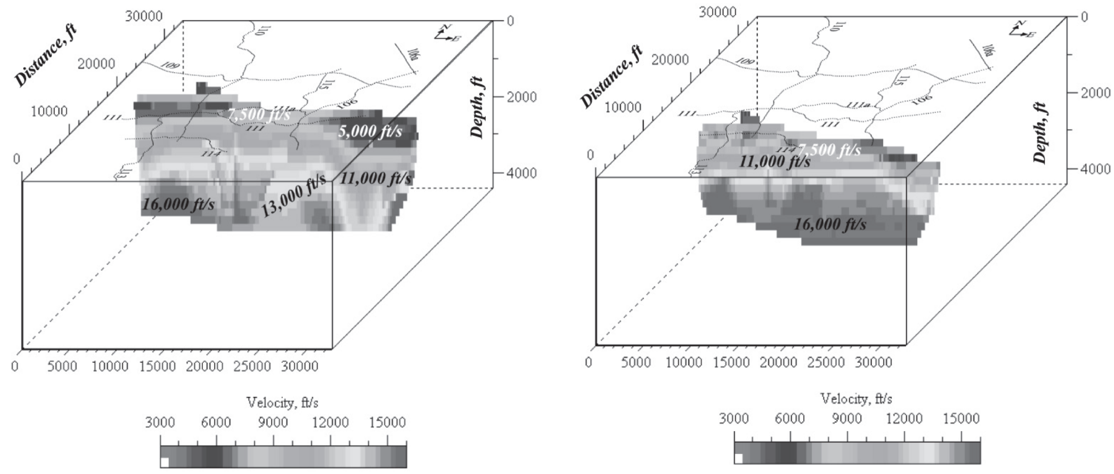

Figure 5. Cross-section through the 3D model obtained during Phase 2.

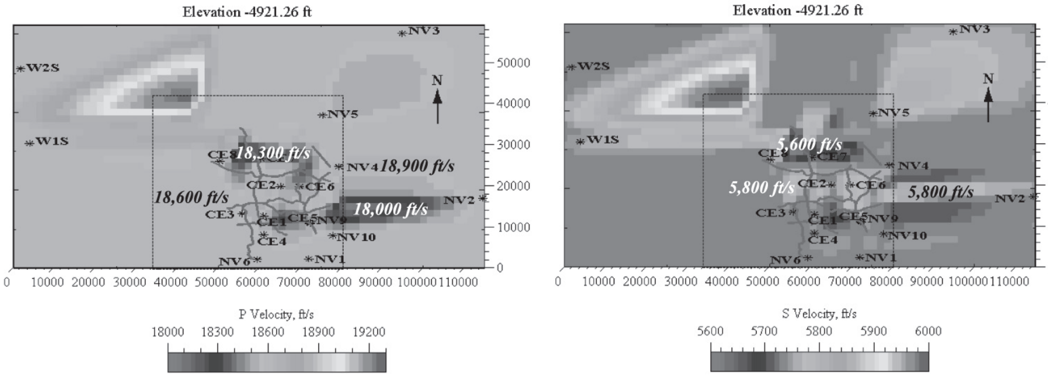

Figure 6. Depth section at elevation of 4920 feet below sea-level showing P-wave (left) and S-wave (right) velocity models obtained using a joint velocity-hypocentral inversion of MEQ data recorded by the Coso MEQ network.

Phase 3

During Phase 3 the refined 3D velocity model obtained during Phase 2 will be used to re-migrate the reflection data to improve the depth sections obtained during Phase 1. The work is on going and results will be presented at the conference.

Conclusions

Analysis of seismic reflection line reveals several important features about the Coso geothermal field. Using MEQ data allows the model to be extended in depth down to 13,000 feet. The velocity models provide useful signatures for geothermal exploration while the depth migrated images provide insights in the local and regional tectonics. Our interpretation of the reflection data supports the hypothesis of Monastero (1997) that the central Coso Range is a modern analog for some exhumed metamorphic core complexes.

References

Asad, A.M., S.K. Pullammanappallil, A. Anooshehpoor, J.N. Louie, 1999. "Inversion of travel time data earthquake locations and three-dimensional velocity structure in the Eureka Valley area, eastern California." Bulletin, Seismic Society of America, v. 89, 796-810.

Lees, J.M., and H. Wu, 2000. "Poisson's ratio and porosity at Coso geothermal area, California." Journal of Volcanology and Geothermal Research, v. 95, p. 157-173.

Monastero, F.C., and J.R. Unruh, 2002. "Definition of the brittle-ductile transition in the Coso geothermal field, east-central California." to be published in the 2002 EAGE Conference volume.

Monastero, F.C., 1997. "Evidence for a nascent metamorphic core complex at the Coso geothermal area, California." EOS (Transactions, American Geophysical Union), v. 78, n. 46, p. F659.

Pullammanappallil, S.K., and J.N. Louie, 1993. "Inversion of seismic reflection traveltimes using a nonlinear optimization scheme." Geophysics, v. 58, p. 1607-1620.

Pullammanappallil, S.K., and J.N. Louie, 1994a. "A generalized simulated-annealing optimization for inversion of first arrival times." Bulletin of the Seismological Society of America, v. 84, p. 1397-1409.

Pullammanappallil, S.K., and J.N. Louie, 1994b. "Regional velocity estimation by simultaneous optimization of earthquake and refraction travel time data." presented at the American Geophysical Union Fall Meeting, San Francisco, California, Dec. 5-9; suppl. to EOS Transactions of the American Geophysical Union, 75, no.44, 425.

Pullammanappallil, S., W. Honjas, J.R. Unruh, and F.C. Monastero, 2001. "Seismic imaging of the Coso geothermal field using advanced data processing techniques." Proceedings, Twenty-Sixth Workshop on Geothermal Reservoir Engineering, Stanford University, Stanford, California, January 29-31, SGP-TR-168.

Unruh, J.R., E. Hauksson, F.C. Monastero, R.J. Twiss, and J. Lewis, 2002. "Seismotectonics of the Coso Range-Indian Wells Valley Region, California: Transtensional Deformation Along the Eastern Margin of the Sierra Nevada Microplate." to be published in Geological Society of America special volume on extensional tectonics of the Indian Wells Valley region

Walker, J.D., and R.W. Whitmarsh, 1998. "A tectonic model for the Coso geothermal area." U.S. Department of Energy Proceedings Geothermal Program Review XVI, April 1-2, Berkeley, California, p. 2-17 to 2-24.

Whitmarsh, R.W., 1997. "New and compiled mapping of the central Coso Range." available in Arcinfo-compatible format from the University of Kansas, Dept. of Geology, Structural Geology and GIS Laboratory (http://geomaps.geo.ukans.edu/html/coso.html);.

William Lettis and Associates and Optim LLC, 2001. "Demonstration of integrated seismic data acquisition and processing techniques for 2D and 3D imaging of structures controlling permeability within the Coso geothermal field, east central California." prepared for US Navy Geothermal Program Office, China Lake, California, Contract number N68936-99-C-0186. p. 98.

Wilson, C. K., C.H. Jones, and H.J. Gilbert, in review, "A single-chamber silicic magma system inferred from shear-wave discontinuities of the crust and uppermost mantle, Coso geothermal area, California." manuscript submitted to the Journal of Geophysical Research.